Effect of Drive Train and Fuel Control Design on Helicopter Handling Qualities

Giorgio Guglieri
Dipartimento di Ingegneria Aeronautica e Spaziale, Politecnico di Torino,
Corso Duca degli Abruzzi, 24, 10129 Torino, Italy

A comprehensive formulation for drive train torsional dynamics is included in a high order mathematical model. The dynamic response is validated for a realistic helicopter configuration. The effects of governor and drive train design parameters on rotorcraft stability in hovering flight are analyzed. Two different mathematical models are considered: a high order blade element type model (34 DOFs) and a reduced order analytical model (8 DOFs). The impact of rpm-governor design parameters on the application of some relevant ADS-33D handling qualities criteria is also evaluated.

Nomenclature

B_1	engine damping
C_T	thrust coefficient
c_ζ	lag damper coefficient
e	hinge offset
I_{eq}	equivalent inertia
I_ζ	blade moment of inertia
K_C	collective anticipation gain
K_D	fuel controller derivative gain
K_I	fuel controller integral gain
K_P	fuel controller proportional gain
$(K_P)_{\xi=0}$	stability limit for fuel controller proportional gain
K_S	torsional stiffness of rotor shaft
k_ζ	lag damper coefficient
M_ζ	blade mass moment
m_ζ	blade mass
n_b	number of blades
Q	shaft torque ($Q = r_g Q_E$)
Q_E	engine torque
Q_0	torque maximum peak after collective input (see Ref. 26 for definition)
Q_1	torque minimum peak after collective input (see Ref. 26 for definition)
R_{2k}	lag force acting on the hinge of the k-th blade
r_g	engine to rotor rpm ratio
r_1	yaw rate due to collective input (see Ref. 26 for definition)
r_3	yaw rate due to collective input (see Ref. 26 for definition)
TPI	Politecnico di Torino
T_Q	torque dynamics derivative
T_{wf}	torque dynamics derivative
T_h	time constant for heave response after collective input
$\mathbf{u}$	control vector
w_f	governor fuel flow rate
w_3	altitude rate after collective input (see Ref. 26 for definition)
$\mathbf{x}$	state vector
β	flap angle of main rotor blade
ζ	lag angle of main rotor blade
θ_{TR}	collective pitch of tail rotor
θ_o	collective pitch of main rotor
θ_{1c}, θ_{1s}	cyclic pitch components
μ	advance ratio
ξ	damping ratio
σ	rotor solidity
τ_{wf}	fuel flow time constant
ψ_b	rotor hub angular displacement
ψ_1	shaft angular displacement at the exit of the gearbox
Ω	main rotor angular velocity ($\Omega = \dot{\psi}_b$)
Ω_1	shaft angular velocity ($\Omega_1 = \dot{\psi}_1$)
ω_n	natural frequency

Introduction

Large rotor speed variations may produce a significant degradation of aircraft handling qualities in maneuvering flight (Refs. 1, 2). The trend towards using lower inertia rotor systems in modern helicopter reduces the level of kinetic energy stored in the system and makes the rotor more susceptible to large variations in its rotational speed during rapid maneuvers.

Severe torsional oscillations in the helicopter rotor drive shaft, and dynamic interface problems involving rotor, drive train and airframe subsystems were also observed in several testing conditions (Refs. 3, 4).

The increase in the responsiveness of the engine/fuel control system using a conventional rotor speed governor can severely compromise the stability margin of the torsional dynamics of the rotor system (Ref. 5). The possible proposed solutions are: either the decoupling of control laws between engine fuel control and airframe/rotor dynamics or the integration of power management into the flight control system.

Presented at the 25th European Rotorcraft Forum, Rome, Italy, September 14–16, 1999. Manuscript received June 1999; accepted September 2000.

Much of the industry experience with rotor/engine dynamics problems is reported in Ref. 6: (i) excessive rotor induced vibration of the propulsion system, (ii) excessive vibration (forced or self-excited) because of engine/drive train/rotor resonances, (iii) engine/drive train torque oscillations, often involving high gain fuel control systems, (iv) excessive rotor overspeed or droop during maneuvers, which is corrected by revising the engine/fuel control system.

All these reference studies demonstrate that the dynamic coupling of engine with fuel control and rpm-governor units is a critical aspect for turbine powered helicopters. As a matter of fact, the coupled rotor/engine/fuel control system dynamics is dominated by responses in two frequency ranges: a low frequency mode of operation that characterizes the fastness of the engine speed response to fuel control inputs, and the higher frequency modes associated with the torsional dynamics of the drive train coupled with blade lag motion.

A discussion of engine control compensation for power turbine speed governing system stabilization is presented in Ref. 7. The results demonstrate that the notch-filter concept may produce excellent transient response characteristics while maintaining good stability margins. The development of new advanced engine control strategies for micro-processor based fuel control systems on a twin engine helicopter is also discussed in Ref. 8. Torsional stability with inoperative rotor blade lag dampers is obtained by incorporating second order notch filtering in the fuel control power turbine governor. An active control strategy is suggested for enhancing drive train stability in Ref. 9.

A parallel research activity in the field of mathematical modeling was developed, with the aim of extending the accuracy of simulations, that may assess the impact of engine/drive train dynamics on the operational effectiveness of the aircraft.

A partial derivatives engine model based on generalized factors was used by Sanders (Ref. 10) to simulate the torque response to fuel inputs. The rotor-engine system was represented by two rotating masses connected by a torsional spring.

The torsional stability of a closed-loop dynamic system (a typical transport helicopter speed governor, gas turbine engine and drive train) is evaluated in Ref. 11.

A flight dynamics simulation tool (Genhel) has been developed in Ref. 12 which treats engine, fuel control, rotor and airframe. This nonlinear mathematical model is adopted in Ref. 13 to investigate the torsional compatibility of the engine/fuel control with helicopter rotor and airframe dynamics at frequencies below the rotational speed.

A simple model, which consists of two masses with a centrifugal spring, assuming a very stiff rotor shaft, is proposed in Ref. 14. The results of eigenvalue analysis and time simulations demonstrate that the rotor speed degree of freedom couples only with the collective lag mode.

A high order mathematical model of a helicopter (UM-Genhel) is described in Ref. 15. The effect of drive train torsional dynamics is not included. The dynamics of the propulsion system affects very little the predictions of the pitch and roll rate frequency responses. The most significant effects of the propulsion system is observed in the vertical acceleration and yaw rate responses.

An alternative approach to the problem of modeling the effects of propulsion system dynamics on handling qualities is proposed in Ref. 16. Drive train torsional dynamics is described by discrete masses and a flexible rotor shaft. This simplified formulation is extremely general and it was found to be accurate for the estimation of the dominant first torsional mode, which is the most important for the integration of engine and airframe.

A blade element model for a hingeless helicopter was developed in Ref. 17. The results confirm that, although the inclusion in the model of drive train degrees of freedom promotes intermodal couplings, pitch and roll short term handling qualities are largely unaffected by propulsion system design.

A complete engine/governor/drive train model was integrated into the DLR B0105 helicopter simulation code SIMH (Ref. 18). With the inclusion of both engine and drive train dynamics, improvement in the dynamic prediction of helicopter shaft torque, rotor speed, heave and yaw motion for collective and pedal inputs could be achieved.

The analysis of references on mathematical modeling shows that engine manufactures tend to use a sophisticated engine dynamic model in conjunction with a rather rudimentary model of helicopter rotor/airframe dynamics when designing the control system. High fidelity models for engine dynamics are accurate but the computational workload is generally high. Another critical aspect is the different time scaling of the two sets of differential equations governing the engine and the airframe response. Furthermore, these nonlinear computer simulations become inadequate for the analysis of helicopter handling qualities requirements when an extremely simplified model of rotor/airframe dynamics is adopted.

On the other hand, helicopter manufacturers have generally used the opposite approach. As a result, the dynamic interface problems that are not anticipated in the design stage can appear later in the flight test phase of a helicopter development program, requiring modifications to fix the problems (Ref. 5).

Therefore, a balance between the two different levels of accuracy is required in order to obtain a comprehensive mathematical model able to represent the influence of fuel control and drive train/propulsion system design parameters on helicopter handling qualities.

Present Work

The objectives of this paper are:

1) To include the formulation developed in Ref. 16 in a high order mathematical model of articulated rotor and helicopter airframe, and to validate the dynamic response for a realistic helicopter configuration.

2) To analyze the effects of governor and drive train design parameters on rotorcraft stability in hovering flight, considering two different mathematical models: a high order blade element type model (34 DOFs) and a reduced order analytical model (8 DOFs).

3) To evaluate the impact of rpm-governor design parameters on the application of some relevant ADS-33D handling qualities criteria, by means of simulations performed with the higher order mathematical model (34 DOFs).

Mathematical Model

The mathematical model developed is a nonlinear blade-element type representation of a single rotor helicopter with rigid fuselage (see Fig. 1).

The main rotor blades are individually modeled as rigid bodies and the coupled flap-lag dynamics is included. The equations of motion of the rotor are formulated and solved in a rotating coordinate system.

No small angle assumption is invoked for aerodynamic angles of rotor and fuselage. The profile aerodynamic loads are calculated using two dimensional blade element theory with table lookup for blade twist and lift/drag coefficients.

The reactions generated by the lag dampers are nonlinear functions of the axial velocity of the damper itself. These terms are obtained following the procedure described in Refs. 12, 19.

The aerodynamics of fuselage and stabilizers is modeled using coefficients derived from wind tunnel data.

A three-state dynamic inflow model (Ref. 20) is used for the main rotor.

The rigid body motion of the aircraft is modeled using six nonlinear force and moment equations and three kinematic relations (Euler

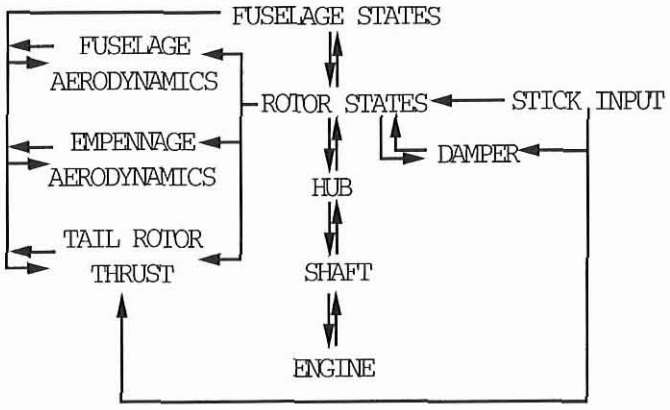

Fig. 1. The flight dynamics simulation model.

equations). The forces and the moments depend on the blade motion and provide the main source of coupling between the rotor and the fuselage. They also contain contributions from fuselage, tail rotor and other aerodynamic surfaces. Both dynamic and aerodynamic rotor-fuselage couplings are included in the model. The latter type of coupling is typically due to the interaction of the rotor wake with the fuselage and tail surfaces, and to the changes of rotor inflow due to the presence of the fuselage. The most important feature of the set of equations of motion for the fuselage used in the present study is that the fuselage states need not be small quantities; thus, all the kinematic nonlinearities associated with the motion of the fuselage are retained.

The propulsion system model is a slightly modified version of that used by Chen (Ref. 16), consisting of discrete masses and a flexible rotor shaft. The equation for engine/drive train torque equilibrium is:

$$I_{eq}\ddot{\psi}_1 + B_1 r_g^2 \dot{\psi}_1 + K_S(\psi_1 - \psi_b) = r_g Q_E$$

The equation for shaft equilibrium is:

$$I_{hub}\ddot{\psi}_b - K_S(\psi_1 - \psi_b) = \sum_{k=1}^{n_b} e \cdot R_{2k}$$

This formulation is more general than that of Ref. 16, which focused on specific rotor modes in which the blades moved in lag only, and with identical angular displacements. The forcing torque is obtained by summing the force contributions R_{2k} of each blade in the hub plane and perpendicular to the root segment of the blade, multiplied by the hinge offset moment arm e. The effects of fuselage angular rates (pitch, roll and yaw rate) on blade dynamics and all the nonlinearities in deriving blade accelerations are retained. Note that the forces R_{2k} also include the terms due to lag dampers.

The order of the complete system is 34 and the state vector $\mathbf{x}$ can be represented as:

$$\mathbf{x} = \begin{Bmatrix} \mathbf{x_F} \\ \mathbf{x_R} \\ \dot{\mathbf{x}}_\mathbf{R} \\ \mathbf{x_I} \\ \mathbf{x_E} \end{Bmatrix}$$

The vector $\mathbf{x_F}$ contains the fuselage degrees of freedom and is defined as

$$\mathbf{x_F} = [u \quad v \quad w \quad p \quad q \quad r \quad \theta \quad \phi \quad \psi]^T$$

The vectors $\mathbf{x_R}$ and $\mathbf{x_I}$ include the rotor and inflow degrees of freedom, transformed in a body-fixed reference system:

$$\mathbf{x_R} = [\beta_o \, \beta_{1c} \, \beta_{1s} \, \beta_{N/2} \, \zeta_o \, \zeta_{1c} \, \zeta_{1s} \, \zeta_{N/2}]^T$$
$$\mathbf{x_I} = [\lambda_o \, \lambda_s \, \lambda_c]^T$$

Finally, the vector $\mathbf{x_E}$ refers to the engine and drive train states:

$$\mathbf{x_E} = [Q_E \, w_f \, \psi_1 \, \Omega_1 \, \psi_b \, \Omega]^T$$

where $\Omega = \dot{\psi}_b$ and $\Omega_1 = \dot{\psi}_1$. The control vector $\mathbf{u}$ is defined as:

$$\mathbf{u} = [\theta_o \, \theta_{1s} \, \theta_{1c} \, \theta_{TR} \, \dot{\theta}_o \, \dot{\theta}_{1s} \, \dot{\theta}_{1c} \, \dot{\theta}_{TR}]^T$$

The presence of time derivatives in $\mathbf{u}$ is required for a correct modeling of the lag dampers (Refs. 12, 19).

The effect of the primary pitch control actuators is also included in the mathematical model and their dynamic response is represented by a second order transfer function (Ref. 19).

The trim procedure is the same as in (Refs. 21, 22). Thus, the rotor equations of motion are transformed into a system of nonlinear algebraic equations using a Galerkin method (10 eqns.). The algebraic equations enforcing force and moment equilibrium (9 eqns.), the additional kinematic equations (2 eqns.) that must be satisfied in forward flight (or in a turn), and the momentum inflow equations for both main and tail rotor (3 + 1 eqns.) are added to the rotor equations, and the combined system (25 eqns.) is solved simultaneously. The solution yields the harmonics of a Fourier series expansion of the rotor degrees of freedom, the pitch control settings, trim attitudes and rates of the entire helicopter, and main and tail rotor inflow.

Flight without sideslip is arbitrarily assumed for $\mu \leq 0.1$, while roll attitude is set to zero for higher airspeed.

The propulsion system is not included in the trim process. This implies two assumptions. The first is that the engine can generate a sufficient torque in any flight condition. The second is that the small fluctuations of rotor speed associated with the lag dynamics of the rotor do not affect the engine torque.

A linearized set of small perturbation equations can be extracted from the nonlinear model:

$$\dot{\mathbf{x}} = [\mathrm{A}] \cdot \mathbf{x} + [\mathrm{B}] \cdot \mathbf{u}$$

The coefficients of the model are derived numerically about the trim condition, using finite difference approximations. The linearization of the rotor equations is carried out in the rotating coordinate system. A multiblade coordinate transformation (i.e. a modal coordinate transformation that is limited to the rotor degrees of freedom) converts the linearized state matrices to a fixed frame (Refs. 19, 23). This transformation only partially reduces the periodicity of the system. Therefore, an averaging of the linearized coefficients evaluated at several positions along the blade azimuth is required.

The response to pilot inputs is obtained from direct numerical integration of the equations of motion. Note that the program is designed for off-line simulation only.

The time responses to fuel flow inputs and rpm-governor dynamics are reproduced with a simplified approach based on the model presented in Ref. 24:

$$\dot{Q}_E = T_Q \Delta Q_E + T_{wf} w_f + K_C T_{wf} \Delta\theta_o$$
$$\tau_{wf} \dot{w}_f = -\Delta w_f + K_D \dot{\Omega} + K_P \Delta\Omega + K_I \int \Delta\Omega$$

The present mathematical model was selected in order to include one time scale only. This simplified model for governor dynamics is based on the assumption that the parameters τ_{wf}, T_Q, T_{wf}, K_P, K_I, K_D and K_C

Table 1. The helicopter configuration

Parameter	Value
Rotor speed	27 rad/s
Rotor disc radius	8.177 m
Blade m.a.c.	0.527 m
Rotor hinge offset e	0.381 m/4.66 %
Blade Lock number γ	7.783
n_b	4
Gross weight	71196 N
CG station/waterline	8.915 m/5.880 m
K_S	541065 Nm/rad
I_{eq}	1673 Kg m^2
I_{hub}	164 Kg m^2
B_1	0 Nm s
r_g	76
K_{D_0}	0 Kg s
K_{P_0}	−0.05397 Kg
K_{I_0}	−0.08246 Kg/s
K_C	0.052 Kg/s
τ_{wf}	0.067 s
T_Q	−7.847 s^{-1}
T_{wf}	61100 Nm/kg

can be identified from real aircraft flight test data for a given flight condition. Although this approach may not be representative of the complete engine/rpm-governor operating range, the complexity of the mathematical model and the number of control parameters is still limited.

Results

The configuration adopted for the numerical simulations is similar to the medium size tactical utility helicopter described in Ref. 12. This aircraft is a single rotor helicopter (Table 1) with articulated flap and lag hinges. The flight condition corresponds to an altitude of 5250 ft in standard atmosphere ($C_T/\sigma \approx 0.081$). The stability augmentation and flightpath stabilization are disabled. The stabilator positions are held fixed at trim setting determined by the numerical computations presented in Ref. 15.

Model validation

System eigenvalues were identified by comparing frequencies and eigenvectors. Propulsion system dynamics enhances intermodal couplings that complicate the identification of poles and normal modes. The related eigenvectors include the engine variables (ψ_b, ψ_1) and their time derivatives. Merging of the fuselage modes is also observed in some flight conditions. Additional modes are introduced in the complete dynamic system (Ref. 16):

1) first torsional mode : this is primarily an engine/shaft motion coupled with blade lag dynamics;

2) second torsional mode : the hub motion is coupled with blade lag dynamics;

The natural frequency of the first torsional mode is quite accurately predicted by the model. The torsional resonance for the real aircraft (Ref. 25) occurs at $\omega_n \approx 17$ rad/s. The first torsional mode is originated by the migration of two lead lag complex conjugate roots, and these eigenvalues migrate back to $\omega_L = \sqrt{(k_\zeta + eM_\zeta\Omega_0^2)/I_\zeta} = 7.222$ rad/s increasing both K_S and I_{eq} (Table 2).

The time response to collective and fuel flow step was also analyzed (Fig. 2). The rpm response is characterized by a sharp deceleration of the engine/drive train system for positive collective step.

Table 2. The first torsional mode in hover

	Without governor		With governor	
Engine param.	ξ (−)	ω_n (rad/s)	ξ (−)	ω_n (rad/s)
$K_S = K_{S_0}$ $I_{eq} = I_{eq_0}$	0.227	17.509	0.160	16.591
$K_S \to \infty$ $I_{eq} \to \infty$	0.452	6.930	0.452	6.946

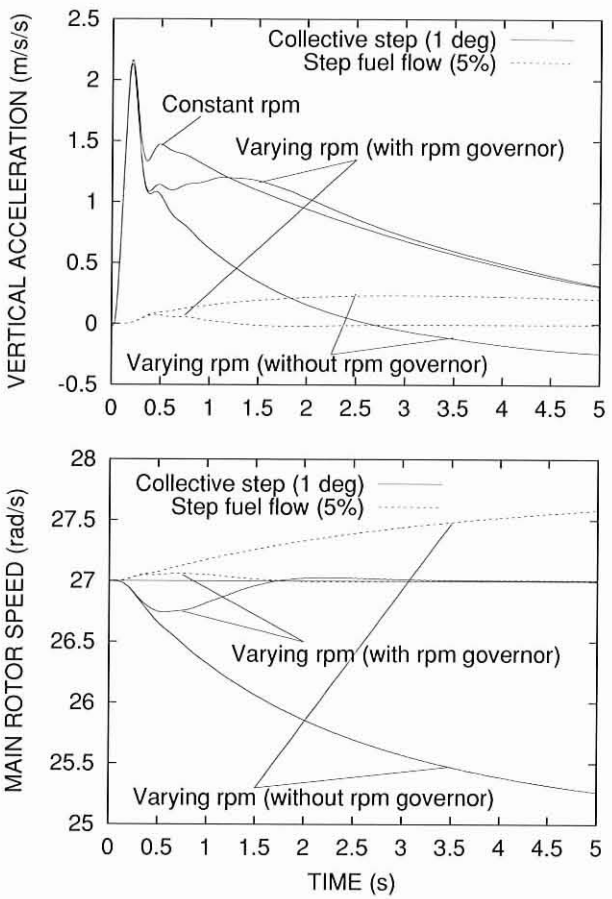

Fig. 2. Vertical acceleration and rpm response to collective step and fuel flow input in hover.

The time history of vertical acceleration is substantially different when engine/drive train dynamics is included. The flattened response for vertical acceleration predicted by the varying rpm model with rpm-governor is confirmed by flight test data (Ref. 16). It is also evident that the constant rotational speed model overpredicts the heave response in the first transient phase. The opposite is verified in the second part of the time history.

Time domain response to collective input ($\dot{\Omega} \neq 0$, $K_P = K_{P_0}$ and $K_I = K_{I_0}$) is also compared in Fig. 3 with dissimilar flight tests performed on a hovering UH-60A helicopter (Ref. 24). The rpm and the fuel flow response were obtained so that the increase of shaft torque due to collective input was the same of flight test data. The rpm variation is quite well reproduced by TPI simulations, although a small discrepancy for initial fuel flow response modeling is observed (also confirmed by the validations presented in Ref. 24).

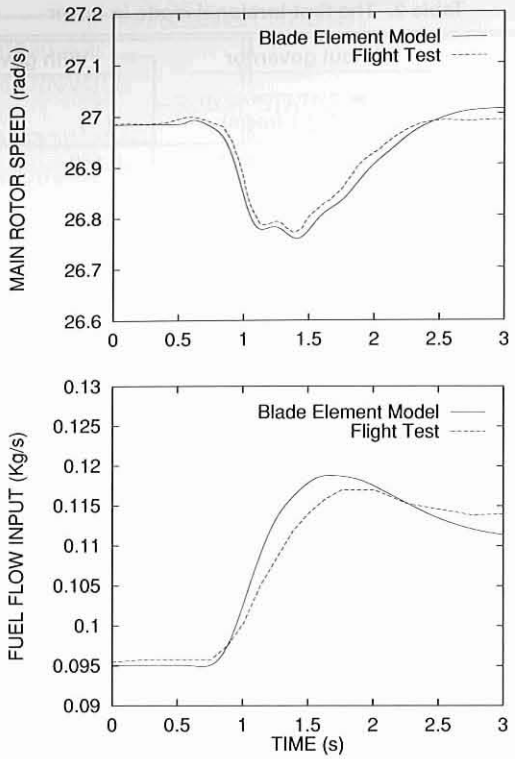

Fig. 3. Response to collective step input in hover: comparison with flight test data.

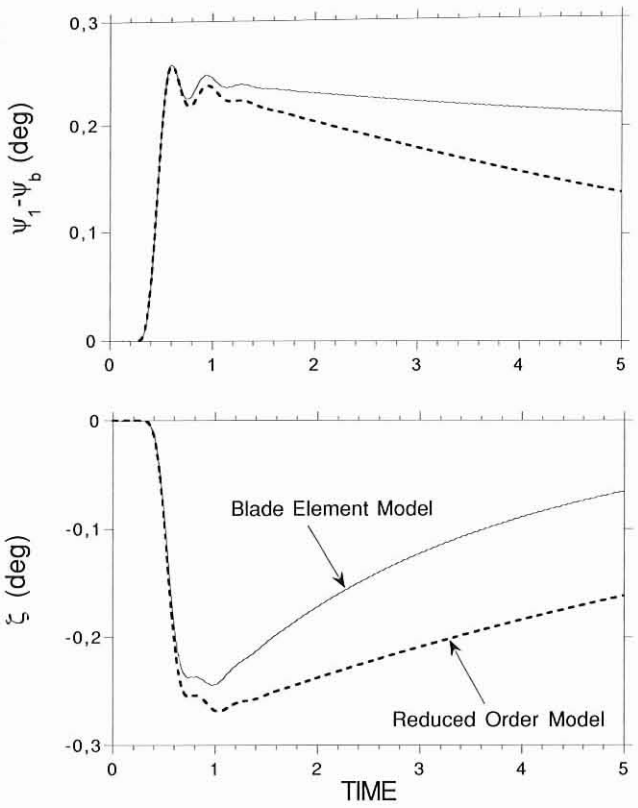

Fig. 4. Comparison of short term open loop response to a step fuel flow input (5%) in hover.

Stability analysis

Two different mathematical models are considered for the stability analysis of the first torsional mode: a high order blade element type model and a reduced order analytical model (the relevant equations are provided in the Appendix). A comparison of open loop time response to step fuel flow input for the complete (34 DOFs) and the reduced model (8 DOFs) is shown in Fig. 4. This comparison demonstrates that short term response (shaft torsion and blade lag) is quite accurately predicted by the low order analytical model.

The effect of shaft stiffness K_S is presented in Fig. 5. The rpm-governor is here disabled ($K_P = K_I = 0$). The increase of stiffness K_S induces an increase of natural frequency for the first torsional mode that is proportional to the square root of the stiffness ratio. The presence of the lag dampers promotes the coupling between flap and lag/shaft modes for the higher order model. This result cannot be reproduced by the reduced order model, where lag dampers are supposed to be decoupled from flap motion and flap dynamics is neglected.

The effect of rpm-governor proportional gain K_P in hovering flight is examined in Fig. 6. The coupling between fuel flow/torque dynamics and drive train is enhanced for higher feedback gains, where the stability of the first torsional mode is compromised. The response to collective input is analyzed with the higher order simulation model in Fig. 7. Both the first and the second torsional mode are excited by the control input. Main rotor angular velocity fluctuations combined with flap and lag oscillations occur when the gain K_P exceeds the stability limit of the first torsional mode.

The unstable behavior is also accurately predicted by the reduced order model and it can be assumed that this last model is able to reproduce the stability degradation due to the increase of fuel flow proportional gain K_P. Hence, a complete analysis of the controller stability boundaries for the

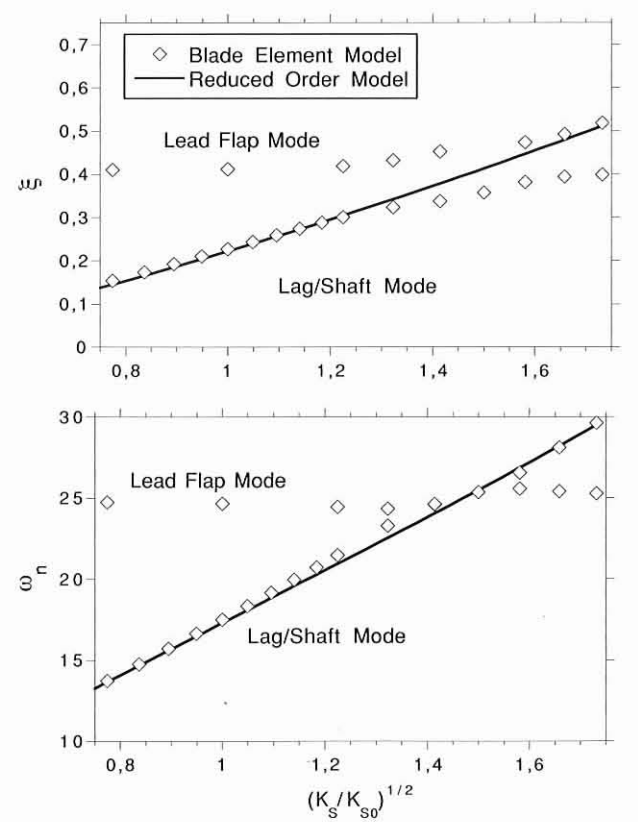

Fig. 5. The effect of shaft stiffness K_S on the first torsional mode in hover.

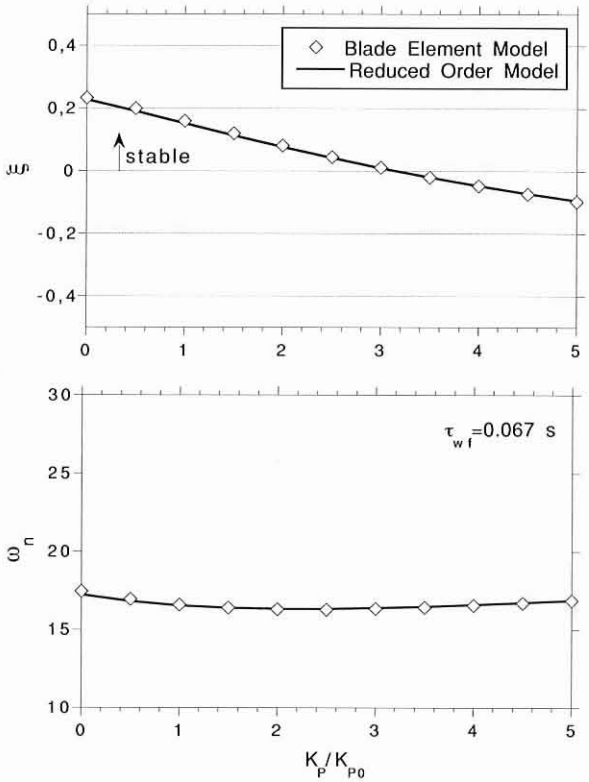

Fig. 6. The effect of fuel controller gain K_P on the stability of the first torsional mode in hover.

first torsional mode was performed assuming that both shaft stiffness K_S and equivalent inertia I_{eq} could be varied within a specified range. This result is presented in Fig. 8 in which the equivalent inertia is normalized with respect to the rotor inertia I_R. The dimensions and the weight of the rotor are held constant. The diagram shows that K_S is the most effective parameter for extending the boundary for acceptable gains K_P within the realistic range of the inertial ratio I_R/I_{eq}.

Furthermore, the decrease of the fuel flow time constant τ_{wf} promotes the reduction of the dynamic stability limit $(K_P)_{\xi=0}$. This result is also confirmed in Fig. 9 where the effects of the parameters K_P and τ_{wf} on torsional dynamics are analyzed. The damping ξ is increased for higher delays while the natural frequency ω_n of the first torsional mode remains fairly constant within the stable range of rpm-governor design parameters.

Handling qualities

The analysis of the impact of rpm-governor design parameters on some relevant ADS-33D handling qualities criteria is considered. The requirements concerning rotor rpm governing in Ref. 26 recommend that the rotational regime of the main rotor should remain within specified limits. Apart from this very general consideration, the effect of the rpm-governor is apparently not considered, assuming that a degradation of drive train stability should probably be detected from the analysis of aircraft handling qualities. A review of the application of the principal criteria for the reference helicopter configuration is here performed in order to verify if any relationship may exist between torsional oscillations and handling qualities criteria. This study is limited to hover as the design parameters for the rpm-governor were identified for that specific flight condition only (Ref. 24).

The frequency domain analysis performed with the higher order model shows that the drive train and rpm-governor design have a limited effect

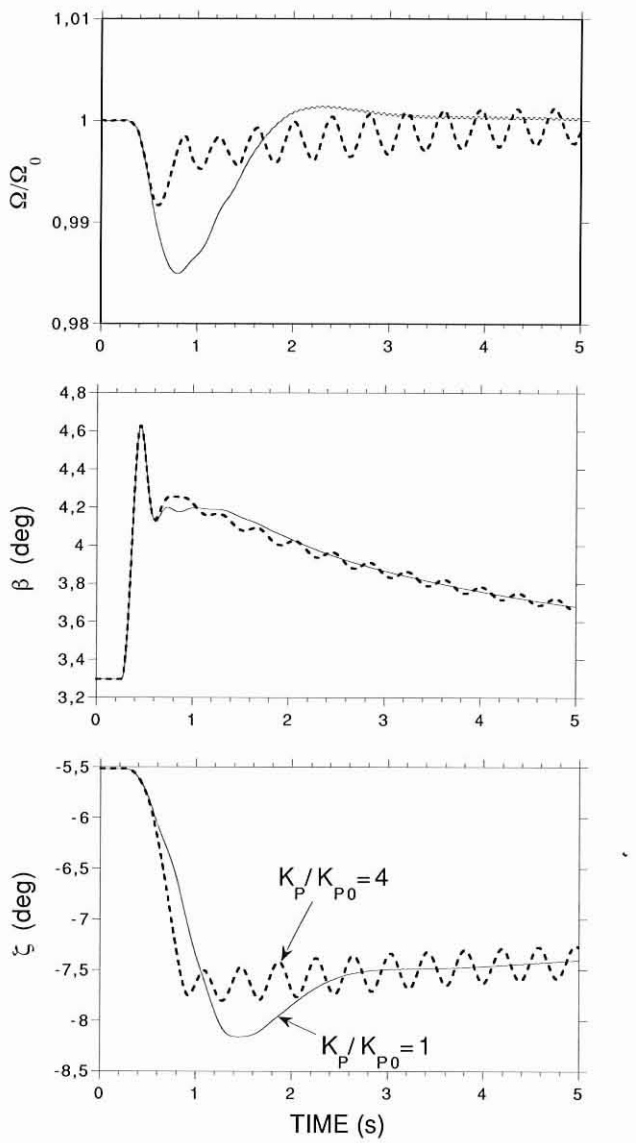

Fig. 7. The effect of proportional gain K_P on the response to collective input (1.6 deg) in hover.

on short term longitudinal and lateral handling qualities. Hence, bandwidth and delay for pitch and roll on-axis response remain fairly constant when governor parameters are modified. Differently, short term directional handling qualities in hovering flight are affected by the coupling between yaw rate and torque, but the effect of K_P and τ_{wf} for the unaugmented aircraft is weak. Note that the model does not include the torsional flexibility of tail rotor transmission.

Time domain response to collective input is analyzed and the mixing of stick inputs is enabled.

Heave response is obviously influenced by rpm-governor design and the most effective parameter is the proportional gain K_P. The effect of K_P on flight path control handling qualities is presented in Fig. 10. The criterion described in Ref. 26 is based on the assumption that the height rate response to a collective step input should have a qualitative first order shape. The increase of rpm-governor proportional gain within the dynamically stable range promotes a reduction of time delay. Differently, when K_P is further increased so that $(K_P)_{\xi=0}$ is exceeded (i.e. when the first torsional mode becomes unstable) no substantial additional reduction of time delay is observed. The time constant $T_h = -1/Z_W$ is

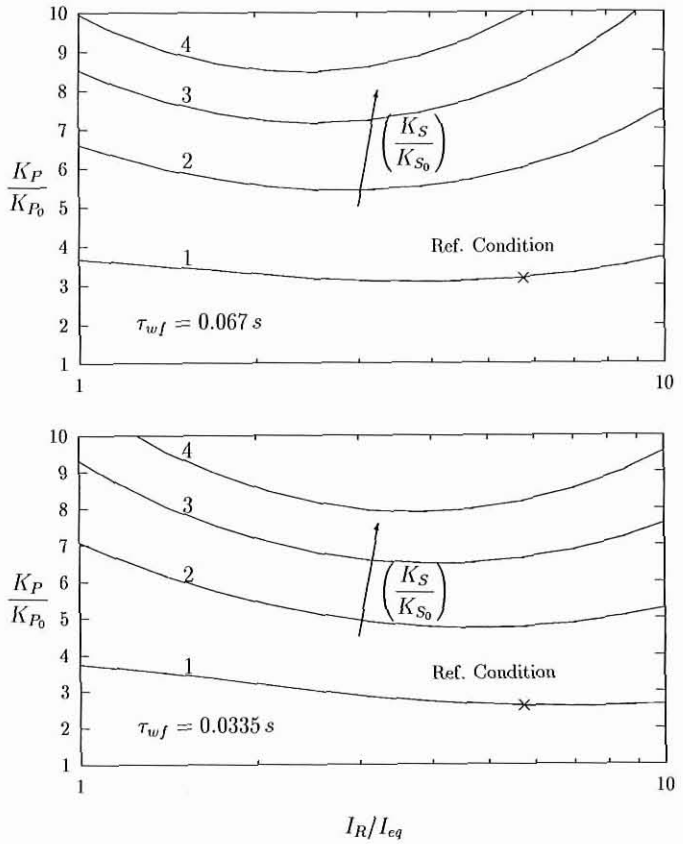

Fig. 8. The stability limit for the fuel controller proportional gain K_P in hover.

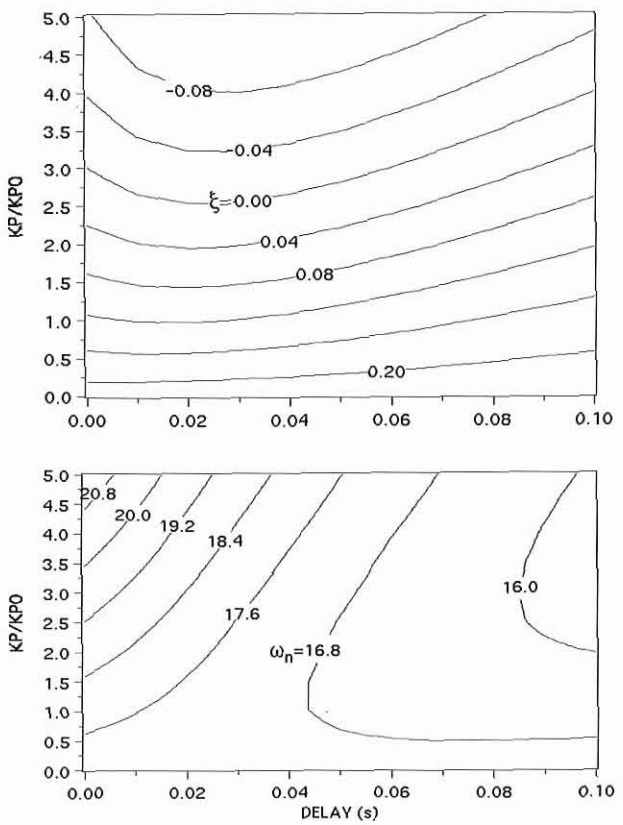

Fig. 9. The effect of fuel controller gain K_P and delay τ_{wf} on the first torsional mode in hover (damping ratio ξ and natural frequency ω_n).

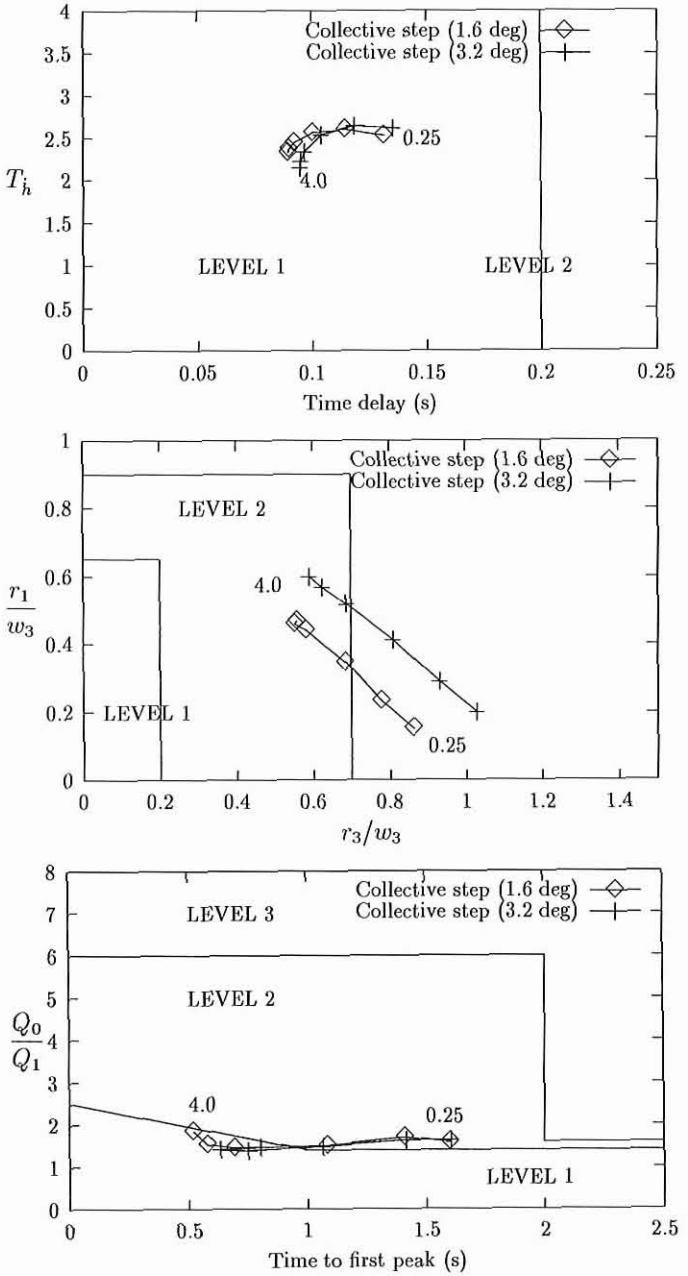

Fig. 10. The effect of proportional gain ($K_P/K_{P_0} = 0.25, 0.5, 1, 2, 3, 4$) on the response to collective input in hover.

marginally influenced by the design of the rpm-governor. An evident change for vertical damping Z_W is only observed for open loop response ($K_P = K_I = 0$).

The criterion for interaxis coupling, i.e. yaw rate response due to collective step input, is presented in Fig. 10. This is the result of the application of a criterion that is based on the estimation of the magnitude of the coupling between heave and yaw rate just after the step control input. An improvement of HQ level is observed for higher feedback gains K_P and apparently drive train torsional instability is not effective in degrading aircraft flying qualities. In order to explain this result the ratio of yaw and vertical rate $r/\dot{h}$ is presented in Fig. 11 for different gain settings. As the proportional gain K_P is increased the transient response is substantially changed and the peak of the ratio between r and $\dot{h}$ is reduced that implies a lower magnitude of the r_3/w_3 coupling parameter (see Fig. 11). Another aspect is the comparison between the constant rpm

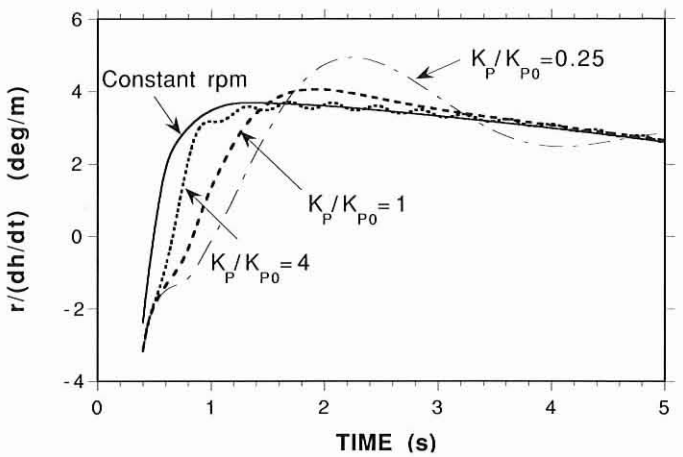

Fig. 11. The effect of fuel controller gain K_P on yaw-heave coupling (1.6 deg step collective input).

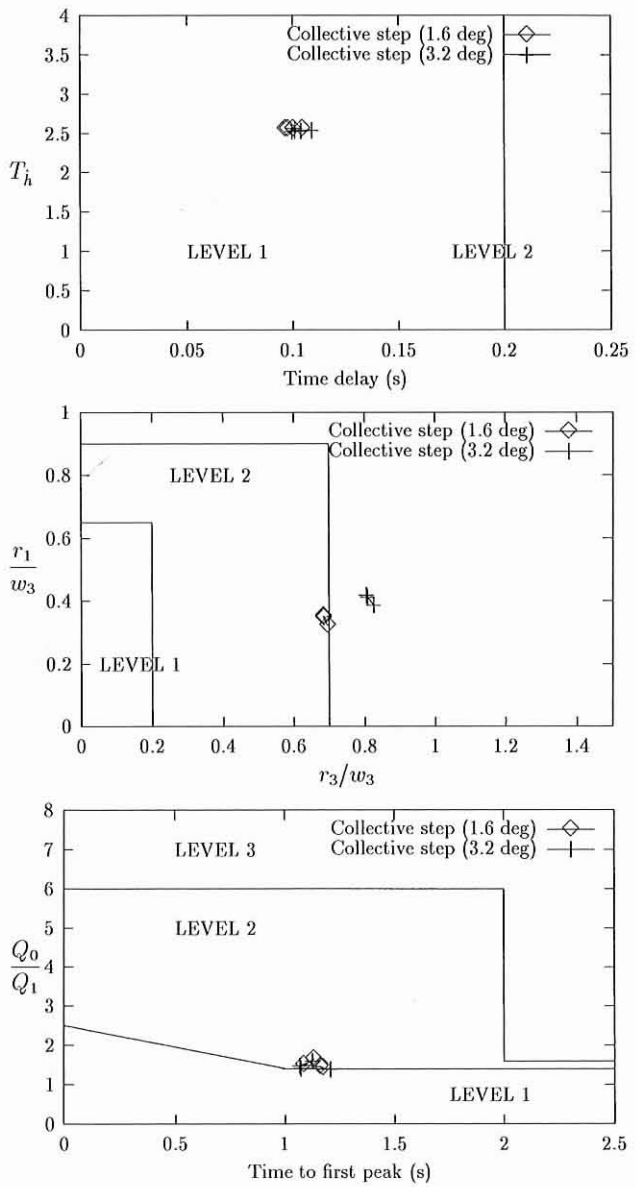

Fig. 12. The effect of delay (τ_{wf}/τ_{wf_0} = 0.25, 0.5, 1, 2) on the response to collective input in hover.

model without torsion of the transmission and the complete model that includes both drive train and rpm-governor dynamics. The former model provides a very smooth response without the typical oscillations in yaw that appear when $K_P \to \infty$ and the slope of $r/\dot{h}$ in the very first transient phase is overpredicted.

The torque response to collective input is analyzed in Fig. 10. The increase of feedback gain promotes a shift of HQ from marginal Level 2 to Level 1 and most of the decrease of time to first torque peak is observed for $K_P < (K_P)_{\xi=0}$. An excess of feedback (i.e. promoting drive train instability) gives a small advantage in terms of torque response while torque oscillations are enhanced.

Finally, the effect of governor delay τ_{wf} on handling qualities is presented in Fig. 12. Higher delays (i.e. a slowed down fuel control) promote drive train stability and do not change the HQ levels of the aircraft in hover.

Concluding Remarks

The formulation developed in Ref. 16 was included in a high order mathematical model of articulated rotor and helicopter airframe, and the dynamic response was validated for a realistic helicopter configuration. The response to collective step input of the real aircraft was quite accurately reproduced.

The effects of governor and drive train design parameters on rotorcraft stability in hovering flight were analyzed, considering two different mathematical models: a high order blade element type model (34 DOFs) and a reduced order analytical model (8 DOFs). This last model was derived reducing to a first order form the equations obtained in Ref. 16 neglecting flap dynamics. Moments from lag dampers were considered and the contributions of torque and rpm-governor dynamics were also included. The reduced order model was found to be accurate for predicting drive train torsional stability and short term dynamic response.

The stability analysis has shown that the presence of the lag dampers enhances the coupling between flap and lag/shaft modes.

The stability of the first torsional mode is compromised for higher feedback gains K_P. The results show that the stiffness K_S is the most effective parameter for extending the boundary for acceptable gains K_P within the realistic range of the inertial ratio I_R/I_{eq}. The damping of the first torsional mode is also increased for higher delays τ_{wf}.

The impact of rpm-governor design parameters on some relevant ADS-33D handling qualities criteria does not reflect the stability degradation of drive train due to high closed loop gains. The application of the specifications given in Ref. 26 is based on the assumption that torsional oscillations should remain within acceptable limits.

Time domain response to collective step input is mainly affected by the increase of the rpm-governor gain K_P and yaw oscillations are present for higher feedback gains. This result is not reproduced by the application of ADS-33D criteria that only reflects the beneficial reduction of both yaw-heave coupling and time to first torque peak.

Heave parameters exhibit higher HQ levels when K_P is increased. This effect is a consequence of lower delays for the heave response to collective step inputs.

Apparently, no specific advantage in terms of flight path control and torque response may derive from excessive feedback.

Higher delays τ_{wf} promote drive train stability and do not change the HQ levels of the aircraft in hover.

Appendix: The Reduced Order Analytical Model

In order to derive a low order approximation for the drive train torsional dynamics, the basic equations obtained in Ref. 16 are reduced to

a first order form and linearized at the reference equilibrium condition ($\Omega = \Omega_1 = \Omega_0$, $\dot{\zeta} = 0$ and $\zeta = \zeta_0$).

The two additional equations presented in Ref. 24 related to the effects of torque and rpm-governor dynamics are also included. Therefore, the reduced order system has 8 degrees of freedom with the following state-space representation $\dot{\mathbf{x}} = [\mathbf{A}] \cdot \mathbf{x}$, and the nonzero elements of the state matrix $\mathbf{A}$ are:

$$a_{12} = 1 \qquad a_{21} = \frac{I_\zeta K_S}{d} \qquad a_{23} = \frac{-I_\zeta K_S}{d}$$

$$a_{25} = \frac{ac}{d} \qquad a_{26} = \frac{-ac_\zeta}{d} \qquad a_{34} = 1$$

$$a_{41} = \frac{K_S}{I_{eq}} \qquad a_{43} = \frac{-K_S}{I_{eq}} \qquad a_{44} = \frac{-B_1 r_g^2}{I_{eq}}$$

$$a_{47} = \frac{r_g}{I_{eq}} \qquad a_{56} = 1 \qquad a_{61} = \frac{-bK_S}{d}$$

$$a_{63} = \frac{bK_S}{d} \qquad a_{65} = \frac{-cI_R}{d} \qquad a_{66} = \frac{c_\zeta I_R}{d}$$

$$a_{77} = T_Q \qquad a_{78} = T_{wf} \qquad a_{81} = \frac{e}{d\tau_{wf}}$$

$$a_{82} = \frac{K_P}{\tau_{wf}} \qquad a_{83} = \frac{-f}{d\tau_{wf}} \qquad a_{85} = \frac{acK_D}{d\tau_{wf}}$$

$$a_{86} = \frac{-ac_\zeta K_D}{d\tau_{wf}} \qquad a_{88} = \frac{-1}{\tau_{wf}}$$

where

$$\mathbf{x} = \left[\int \Delta\Omega \Delta\Omega \int \Delta\Omega_1 \Delta\Omega_1 \Delta\zeta \dot{\zeta} \Delta Q_E \Delta w_f \right]^T$$

and

$$a = -n_b \cdot (I_\zeta + eM_\zeta)$$
$$b = -(I_\zeta + eM_\zeta)$$
$$c = -\left(eM_\zeta \Omega_0^2 + k_\zeta\right)$$
$$d = ab - I_R I_\zeta$$
$$e = f + K_I d$$
$$f = I_\zeta K_S K_D$$
$$I_R = I_{hub} + n_b \cdot \left(I_\zeta + 2eM_\zeta + m_\zeta e^2\right)$$

The model is derived neglecting the effects of blade aerodynamics and assuming that the damper lag reaction ΔQ_ζ on the generic blade can be linearized ($\Delta Q_\zeta = c_\zeta \cdot \dot{\zeta} + k_\zeta \cdot \Delta\zeta$). For the reference helicopter the lag damper damping ratio is $\zeta_D = c_\zeta / 2\sqrt{(k_\zeta + eM_\zeta \Omega_0^2) I_\zeta} \approx 0.396$.

References

[1]Kelley, H. L., Pegg, R. J., and Champine, R. A., "Flying Quality Factors Currently Limiting Helicopter Nap-of-Earth Maneuverability as Identified by Flight Investigation," NASA-TN-D-4931, 1968.

[2]Corliss, L. D., "Effects of Engine and Height Control Characteristics on Helicopter Handling Qualities," *Journal of the American Helicopter Society*, Vol. 28, (3), July 1983.

[3]Warmbrodt, W., and Hull, R., "Development of a Helicopter Rotor/Propulsion System Dynamics Analysis," AIAA/SAE/ASME 18th Joint Propulsion Conference, Cleveland, USA, 1982.

[4]Fredrickson, C., Rumford, K., and Stephenson, C., "Factors Affecting Fuel Control Stability of a Turbine Engine/Helicopter Rotor Drive System," *Journal of the American Helicopter Society*, Vol. 16, (1), January 1972.

[5]Chen, R. T. N., and Mihaloew, J. R., "Rotorcraft Flight Propulsion Control Integration," *Vertiflite*, Vol. 30, (6), 1984.

[6]Johnson, W., "Recent Developments in the Dynamics of Advanced Rotor Systems," AGARD-LS-139, 1985.

[7]Alwang, J. R., and Skarvan, C. A., "Engine Control Stabilizing Compensation Testing and Optimization," *Journal of the American Helicopter Society*, Vol. 22, (3), July 1977.

[8]Howlett, J. J., Morrison, T., and Zagranski, R. D., "Adaptive Fuel Control for Helicopter Applications," *Journal of the American Helicopter Society*, Vol. 29, (4), October 1984.

[9]Krysinski, T., "Active Control of Aeromechanical Stability," AGARD-CP-592, 1996.

[10]Sanders, J. C., "Influence of Rotor Engine Torsional Oscillation on Control of Gas Turbine Geared to a Helicopter Rotor," NACA-TN-3027, 1953.

[11]Darlow, M. S., and Vance, J. M., "Torsional Stability Analysis of a Gas Turbine Powered Helicopter Drive System," ASME Gas Turbine Conference, Zurich, Switzerland, 1974.

[12]Howlett, J. J., "UH-60A Black Hawk Engineering Simulation Program: Volume I—Mathematical Model," NASA-CR-166309, 1981.

[13]Kuczynski, W. A., Twomey, W. J., and Howlett, J. J., "The Influence of Engine/Fuel Control Design on Helicopter Dynamics and Handling Qualities," American Helicopter Society 35th Annual Forum, Washington, DC, USA, May 21–23, 1979.

[14]Ockier, C. J., "Engine-Rotor Interaction: A Dynamic Analysis in Hover," MS Thesis, University of Maryland, 1990.

[15]Kim, F. D., "Formulation and Validation of High Order Mathematical Models of Helicopter Dynamics," Ph.D. Dissertation, University of Maryland, 1991.

[16]Chen, R. T. N., "An Exploratory Investigation of the Flight Dynamic Effects of Rotor RPM Variations and Rotor State Feedback in Hover," NASA-TM-103968, 1992.

[17]Guglieri, G., Celi, R., and Quagliotti, F. B., "Effect of Propulsion System Dynamics on Rotorcraft Aeromechanical Stability in Straight and Turning Flight," AGARD-CP-592, 1996.

[18]Hamers, M., and von Grunhagen, W., "Dynamic Engine Model Integrated in Helicopter Simulation," Twenty-Third European Rotorcraft Forum, Dresden, Germany, September 16–18, 1997.

[19]Kim, F. D., Celi, R., and Tischler, M. B., "High-Order State Space Simulation Models of Helicopter Flight Mechanics," *Journal of the American Helicopter Society*, Vol. 38, (4), October 1993.

[20]Peters, D. A., and HaQuang, N., "Dynamic Inflow for Practical Applications," *Journal of the American Helicopter Society*, Vol. 33, (4), October 1988.

[21]Celi, R., "Hingeless Rotor Dynamics in Coordinated Turns," *Journal of the American Helicopter Society*, Vol. 36, (4), October 1991.

[22]Chen, R. T. N., and Jeske, J. A., "Kinematic Properties of the Helicopter in Coordinated Turns," NASA-TP-1773, 1981.

[23]Johnson, W., *Helicopter Theory*, Dover Publications, New York, 1994, pp. 349–361.

[24]Fletcher, J. W., "A Model Structure for Identification of Linear Models of the UH-60 Helicopter in Hover," NASA-TM-110362, 1995.

[25]Mihaloew, J. R., Ballin, M. G., and Ruttledge, D. C. G., "Rotorcraft Flight Propulsion Control Integration: An Eclectic Design Concept," NASA-TP-2815, 1988.

[26]"Aeronautical Design Standard ADS-33D Handling Qualities Requirements for Military Rotorcraft," U. S. Army Aviation and Troop Command, St. Louis, MO, 1994.